Diamond & Related Materials 66 (2016) 206–212

Contents lists available at ScienceDirect

Diamond & Related Materials

journal homepage: www.elsevier.com/locate/diamond

Surface patterning of synthetic diamond crystallites using nickel powder

Junsha Wang [a,b], Long Wan [a,*], Jing Chen [a], Jiwang Yan [b]

[a] College of Materials Science and Engineering, Hunan University, Hunan 410082, PR China
[b] Department of Mechanical Engineering, Keio University, Yokohama 223-8522, Japan

ARTICLE INFO

Article history:
Received 30 November 2015
Received in revised form 15 April 2016
Accepted 26 April 2016
Available online 02 May 2016

Keywords:
Synthetic diamond crystallites
Surface patterning
Etch patterns
Nickel powder
Graphitization

ABSTRACT

Nickel powder (Ni) was used as catalyst to form micropatterns on diamond crystallites surface without flowing hydrogen gas. Anisotropic etch patterns on {100} and {111} planes of diamond and the interface of diamond and nickel were analyzed, and the pattern area and etch depth formed at different temperatures were measured quantitatively. Results show that the etch patterns on {100} planes were formed as reversed pyramids, while those on {111} planes were hexagons. Compared to {111} planes, {100} planes had better affinity for nickel. And the formation of cubic nanoparticles on the bottom of the patterns might have been caused by the melting and crystallization of eutectic. An increase in temperature promoted the surface patterning process. At the same temperature, {100} planes were etched more significantly than {111} planes in terms of larger pattern area and deeper etch depth. At 950 °C, the average percentages of pattern area on {100} and {111} planes were 21% and 9%, and the corresponding etch depths were 5.0 μm and 3.0 μm, respectively. Moreover, it was demonstrated that graphitization was the dominant mechanism of the diamond surface patterning process.

1. Introduction

Owing to the advantages in hardness, wear resistance, potential range and chemical stability, diamond has been widely used in precision manufacturing industries [1,2] and biological detection field [3,4]. To increase the surface area or introduce nanopores in two-dimensional diamond film used for electrodes or sensors, much attention has been drawn on diamond surface etching by metals in flowing hydrogen gas. Nickel nanoparticles were prepared on the surface of boron-doped diamond (BDD) by vacuum deposition followed by heat treatment in flowing gas of H_2/N_2 [5]. When Ni/BDD was heated at 700 °C for 2 h, Ni nanoparticles were finely dispersed on BDD surface, but no excavation behavior was observed. However, after the temperature climbed to 900 °C, the surface layer of BDD was excavated vigorously and the excavation degree increased with the heating time. Cyclic voltammogram of BDD shows that the surface area reflected by specific capacitance was enhanced by nearly 15 times through the excavation at 900 °C for 24 h. To achieve pores with controlled shape, diamond oriented in different orientations was selected to be etched by molten Ni particles [6]. After heat treatment, reversed pyramids, channels and triangles were formed on {111}, {110} and {100} planes, respectively. And {111} planes, the most resistant to be etched, were shown to be the stopping planes in etch pits. During such a process, the catalytic gasification of carbon with the help of hydrogen was the mechanism of diamond etching [7].

To create etch pits on surface of polyhedral diamond crystallites used as optical material, cobalt were loaded on diamond surface by impregnation in the nitrate solution [8]. After being heated in H_2/N_2, etch pits similar to those on diamond film were achieved. Using the same method, diamond was etched by iron and iron carbide was probably formed in the process [9]. Although a modicum of success has been attained in diamond etching, the process requires hydrogen as a flowing gas. Most importantly, there is little quantitative analysis about the effect of temperature on the etching extent of diamond. Allowing for the processing cost and safety, we developed a new diamond etching method without flowing hydrogen gas [10]. The feasibility of etching behavior of iron on diamond has been verified, but etch pits were not available on the {111} planes. In this paper, nickel powder was used as the catalyst to etch diamond crystallites. Surprisingly, anisotropic etch patterns were found on {100} and {111} planes. After metal was removed by acid, the pattern area and etch depth on diamond surface were quantified by white light interferometer and laser-probe surface profiling, respectively.

2. Experimental

Synthetic diamond crystallites (LD240) with an average diameter of ~500 μm were bought from Henan Liliang New Material Co., Ltd. And nickel powder with size distribution of 12–52 μm was bought from Zhuzhou Cemented Carbide Group Co., Ltd. To start the experiment, diamond and nickel were mixed in a mass proportion of 1:13. Then the mixtures were wrapped by graphite paper and buried in a graphite crucible full of carbon black. In order to build a closed chamber free from air, the graphite crucible was put into an airtight ceramic crucible with carbon black around. Finally, ceramic crucible was heated in the muffle furnace at a rate of 3 °C/min to 600 °C followed by 2 °C/min to750 °C and

* Corresponding author.
E-mail address: wanlong1799@163.com (L. Wan).

http://dx.doi.org/10.1016/j.diamond.2016.04.010
0925-9635/

1.5 °C/min to the objective temperature and then was retained for one hour. After the heat treatment, diamond was washed by the mixed acid of HCl/HNO_3 to remove the metal.

The surface morphology and element distribution of processed diamond were examined by environment scanning electron microscopy (ESEM, FEI, Inspect S50) and energy dispersive X-ray spectroscopy (EDX, Bruker, XFlash Detector 4010). The structural changes of diamond and nickel were analyzed by micro-Raman spectroscopy (JASCO Corporation, NRS-3100YM, laser wavelength: 532 nm, spectral magnification: ×100, NA: 0.95, laser spot size: 1 μm) and X-ray diffraction (XRD, Bruker, D8 Advance) with Cu K radiation. The area and depth of patterns on diamond were quantified using white light interferometer (Taylor Hobson Ltd., CCI 1000) and laser-probe surface profiling (Mitaka Kohki Corporation, MP-3), respectively.

3. Results and discussion

3.1. Morphology observation

Fig. 1 shows the ESEM images of Ni-patterned diamond crystallites at different temperatures. When the heat-treatment temperature was 700 °C, micron-sized mutually orthogonal channels aligned in ⟨100⟩ direction were observed on {100} planes. However, at the ends of channels (indicated by a circle in Fig. 1(a2)), the orientations of sides

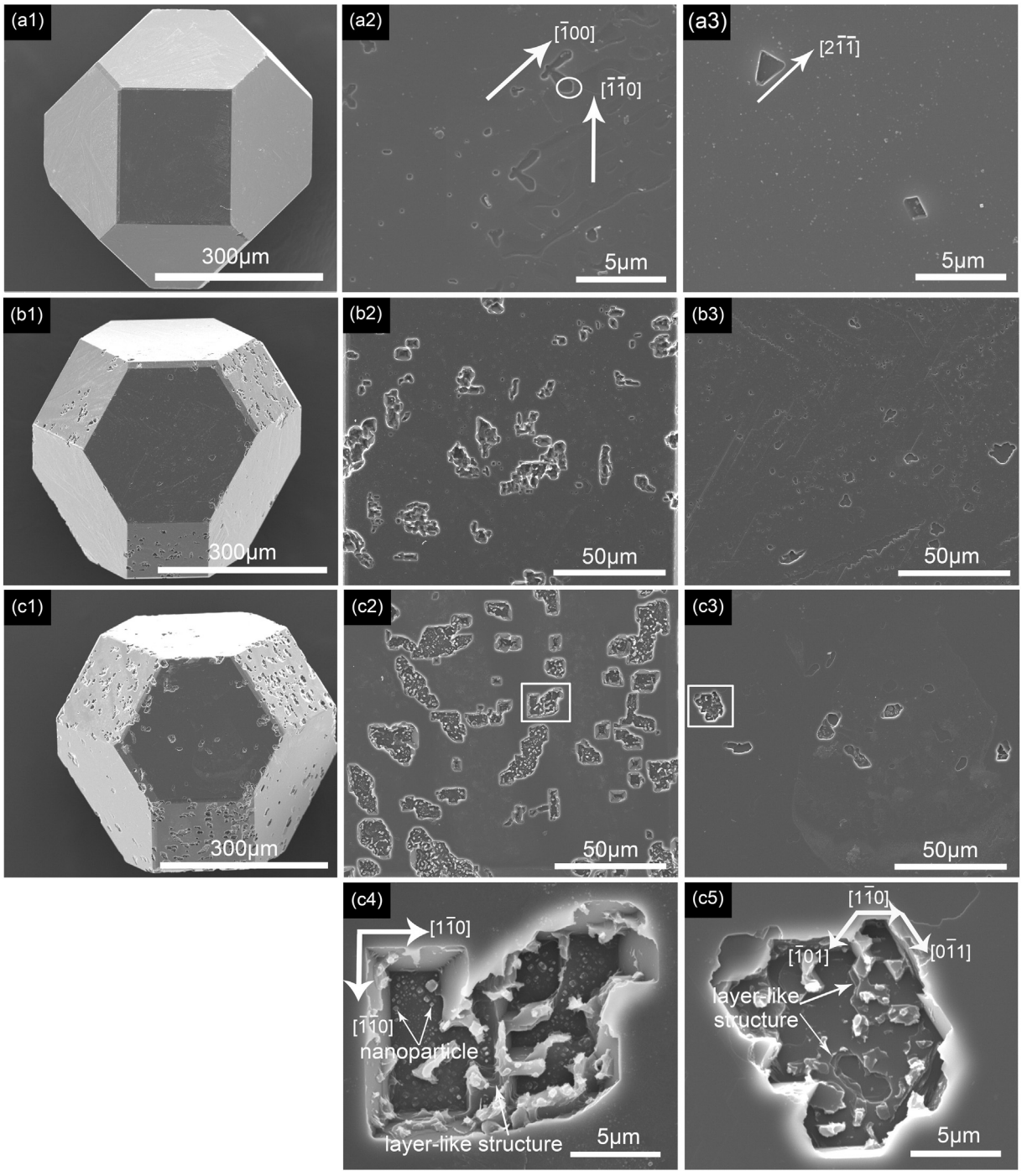

Fig. 1. Morphology of Ni-patterned diamond crystallites heated at (a1) 700 °C, (b1) 800 °C and (c1) 900 °C. ((a2), (b2) and (c2) are the corresponding {100} planes; (a3), (b3) and (c3) are the corresponding {111} planes; (c4) and (c5) are the enlarged square parts in (c2) and (c3), respectively.).

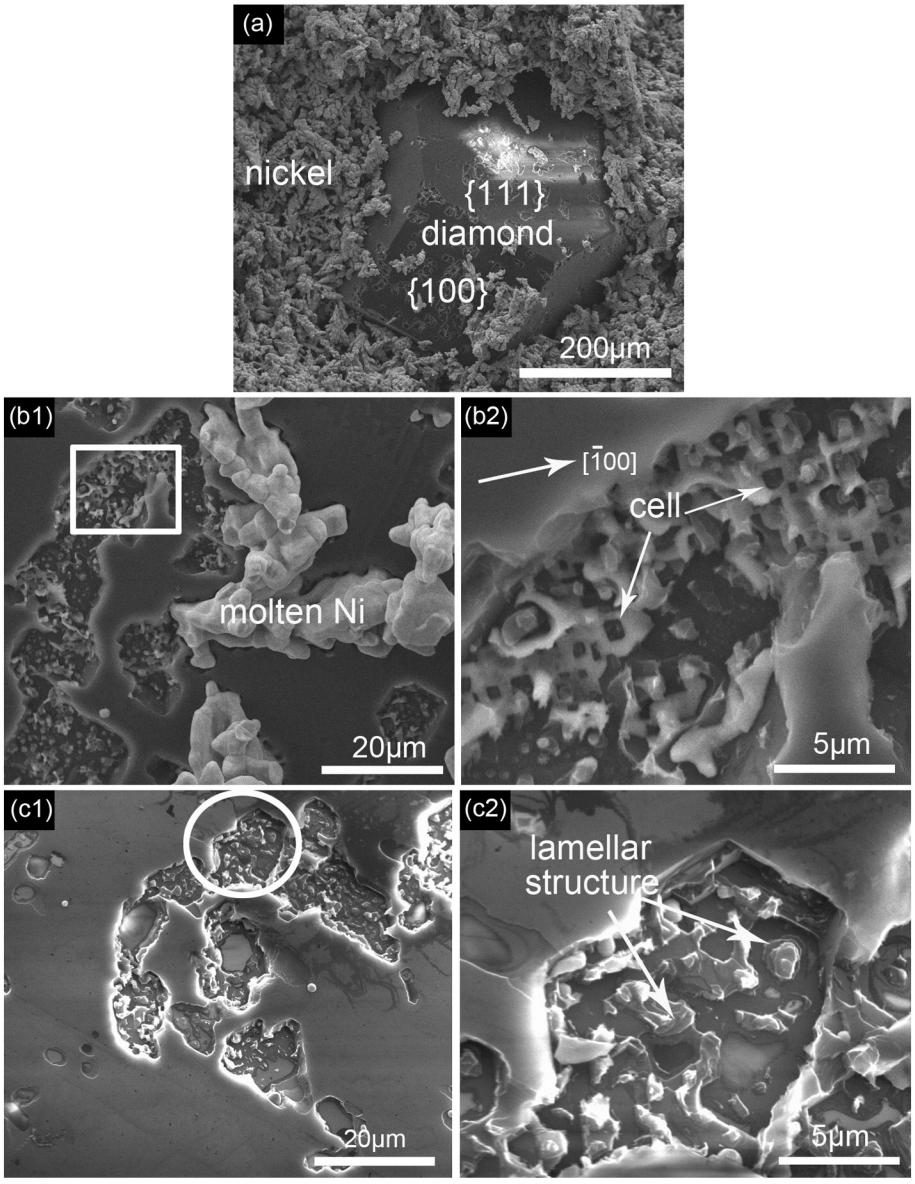

Fig. 2. ESEM images of (a) fracture surface of diamond/nickel bulk; (b1) {100} planes; (b2) enlarged square part in (b1); (c1) {111} planes; and (c2) enlarged circle part in (c1).

rotated 45° and became to be along ⟨110⟩ direction. While on {111} planes, triangles with edges oriented in ⟨2 − 1 − 1⟩ direction were formed. It seems that the formation of etch patterns originated from the orientations with lower atom density. When the temperature went up to 800 °C, obvious etch patterns were developed on diamond surface. Compared to {111} planes, the pattern area and etch depth on {100} planes were much larger. The same situation continued after diamond was etched at 900 °C. On {100} planes, etch pits or channels with flat bases and smooth {111}-oriented sidewalls were observed (shown in Fig. 1(c4)). Whereas on {111} planes, etch patterns were the combination of hexagons (shown in Fig. 1(c5)). It was also noteworthy that the edges of etch patterns on both {100} and {111} planes were along ⟨110⟩ direction which were parallel to the edges of the etched plane. Furthermore, layer-like structure was seen in etch patterns indicating that diamond was etched away via a step mechanism.

To shed light on the interface between diamond and nickel, the fracture surface of diamond/nickel bulk heated at 900 °C are shown in Fig. 2. It is seen that at a temperature lower than the melting point (1455 °C) of nickel bulk, micron-sized Ni particles were melted, which might be attributed to the particle size effect. In this case, the melting point of metal particles generally declines with the decrease in particle size

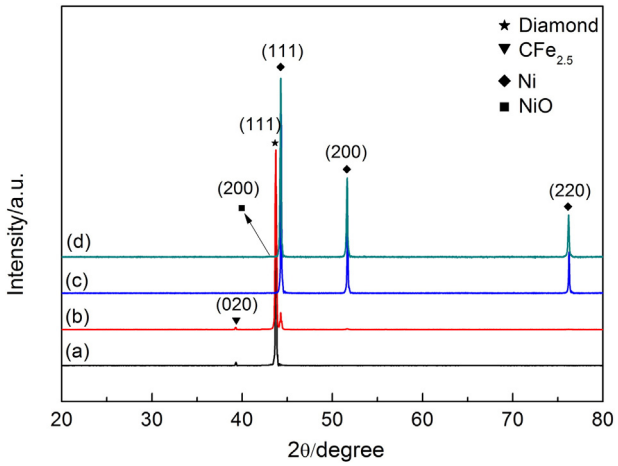

Fig. 3. XRD patterns of (a) pristine diamond; (b) Ni-patterned diamond before acid wash; (c) pristine nickel powder and (d) nickel powder separated from diamond/nickel bulk after experiment.

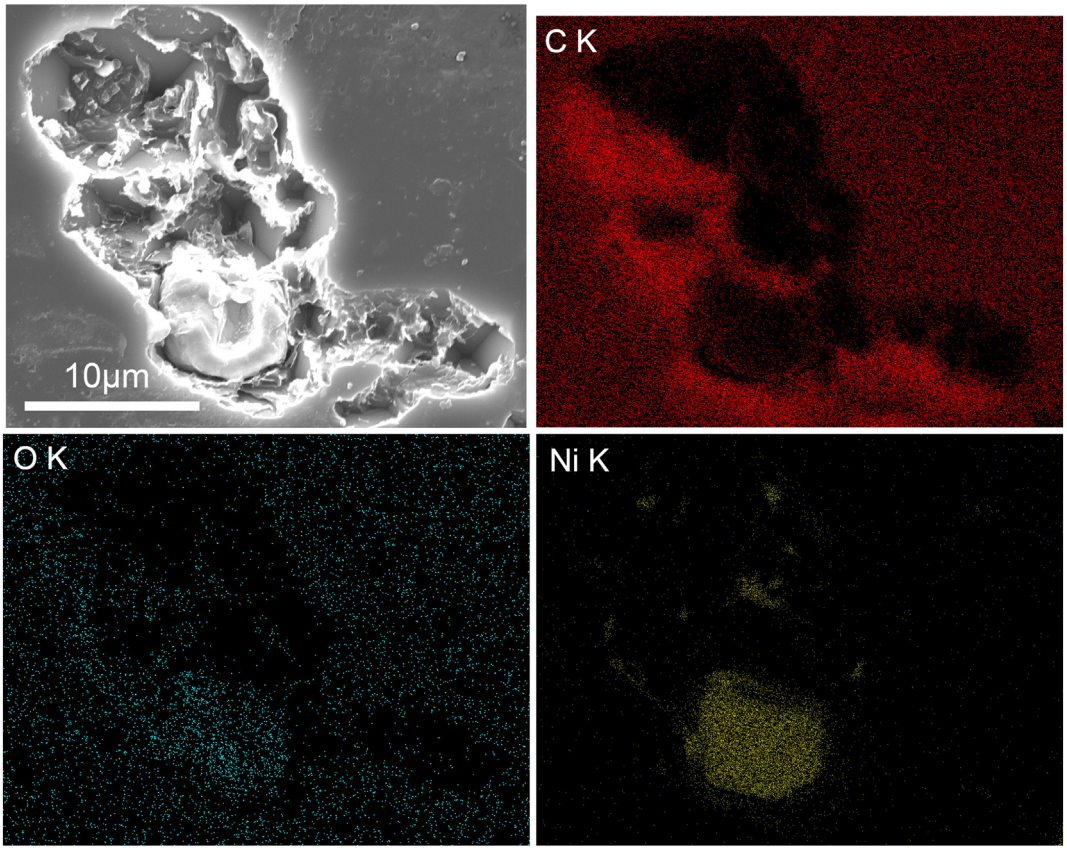

Fig. 4. Element distribution on the Ni-patterned {100} planes at 900 °C.

[11]. On {100} planes, apart from etch patterns corresponding to the zone where metal was removed, interface formed due to the adhesion of nickel to diamond surface was also observed in Fig. 2(b2). It is very interesting to note that the resultant structure was characterized by cells with walls oriented in ⟨100⟩direction. After the nickel was washed away by acid, the cubic nanoparticles were left on the bottom of etch patterns (Fig. 1(c4)). From the brightness contrast with diamond and the orientation difference from {100} planes, those nanoparticles might have been caused by the melting and crystallization of melt [12]. If so, the existence of metastable eutectic will also contribute to the formation of the molten phase [13]. Apparently being different from {100} planes, adhered nickel was seldom observed in etch patterns on {111} planes (shown in Fig. 2(c2)). This phenomenon, from another side, gave the evidence that {100} planes has better affinity for nickel

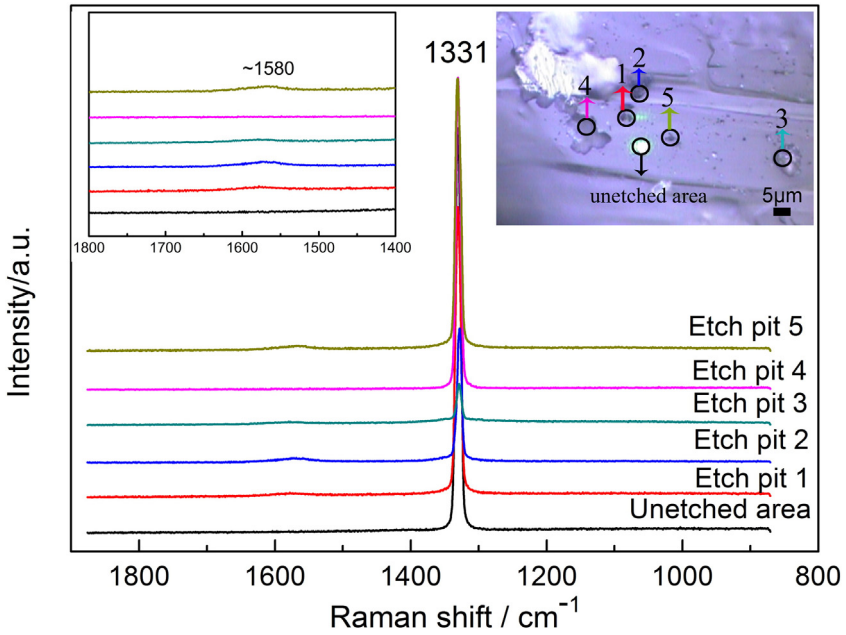

Fig. 5. Micro-Raman spectra of unetched area and etch pits on Ni-patterned {100} planes before acid wash. (The inset in the right corner is the optical micrograph of {100} surface for indicating the position of etch pits.)

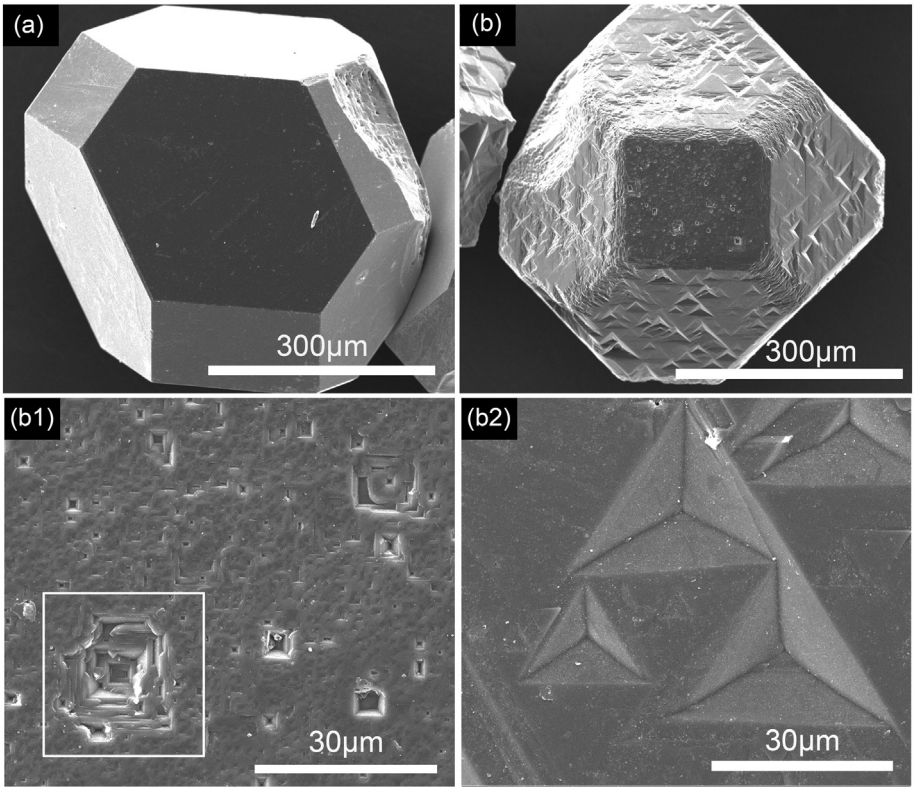

Fig. 6. Morphology of diamond: (a) diamond with carbon black covered was heated at 900 °C; and (b) diamond and nickel exposed in air was heated at 900 °C. ((b1) and (b2) are {100} planes and {111} planes corresponding to (b).)

than {111} planes [14]. Furthermore, because of the incomplete etching, irregular lamellar structure was retained on the bases of etch patterns. Nevertheless, if the etching proceeded ideally layer by layer, the bottom of etch patterns on {111} planes should be perfectly smooth and flat. This feature, on the contrary, is unavailable for {100} planes, which is determined by the property of the crystal planes [15].

3.2. X-ray diffraction (XRD) and element mapping analysis

Fig. 3 compares the XRD patterns of diamond and nickel powder before and after surface patterning experiment. It is shown that the *as*-received diamond crystallites had inclusion of iron carbide ($Fe_{2.5}C$). Whereas, the pristine nickel powder used in the experiment did not have any impurity of nickel oxide. After the surface patterning experiment at 900 °C, pure Ni was detected on diamond surface but no graphite or nickel carbide. Similarly, nickel powder separated from diamond/nickel bulk was also mainly pure Ni. But at the same time, the strongest diffraction peak of NiO corresponding to (200) facet was identified. Considering that the NiO peak is very weak, the amount of oxygen should be quite little. To demonstrate its existence further, element mapping was done on Ni-loaded {100} planes (shown in Fig. 4).

In Fig. 4, the oxygen element (O) was found to concentrate in the Ni located area. Being affected by the measurement noise, the unetched area of {100} planes was also covered by O element. In this sense, only quite little amount of nickel powder in etch patterns was oxidized, which is consistent with the XRD result (the effect of oxygen on the etching process will be discussed in the following part). Moreover, slight C element was detected in etch patterns especially in the Ni-rich zone, which might derive from graphite carbon dissolved in nickel.

3.3. Raman spectrum of diamond surface

To confirm the phase of carbon in etch patterns in Fig. 4, unpatterned area and etch patterns on {100} planes were examined using micro-Raman (as shown in Fig. 5). As expected, unetched area was only characterized by a sharp diamond peak at about 1331 cm^{-1} [16]. In contrast, graphite carbon peak at around 1580 cm^{-1} [17] was identified in most of tested etch patterns with or without nickel covered. That is to say, phase transformation from diamond to graphite was involved in the diamond patterning process.

In Nickel structure (Fig. 1S), the edge length of the equilateral triangle formed by the three adjacent atoms on (111) plane is 2.49 Å. While that of three atoms in diamond structure is 2.52 Å. Because their edge lengths are very close, Ni atoms on (111) plane can be vertically aligned with diamond atoms. As shown in Fig. 2S [18], three Ni atoms are vertically aligned with diamond atom 1, 3, 5. With two unpaired d electrons, Ni atoms will attract electrons of diamond atom 1, 3, 5 and simultaneously compress atom 2, 4, 6. Then, diamond structure is converted to hexagonal graphite structure with the inner triangle length is 2.46 Å.

3.4. The effect of oxygen on the surface patterning process

From the results of XRD and element mapping, a little of nickel oxide was identified. It might be formed during the surface patterning process or during the sample preservation process after experiment. If the oxidization of nickel existed in the experiment process, the slight oxygen should come from the sample preparation process. To make clear whether such tiny amount of oxygen will contribute to the patterning process or not, diamond crystallites buried in the carbon black were heated at 900 °C. As a result, little changes were seen on diamond surface (Fig. 6(a)). It proves that the oxygen here cannot cause the oxidization of diamond itself.

On the other hand, the mixture of diamond and nickel was exposed in the air and then heated at 900 °C. After the interaction among air, nickel and diamond, {100} planes of diamond lost their original surface and became very rough. A big etch pit (indicated by square in Fig. 6(b1)) was shown to be reversed pyramid with interlaced steps, which was also reported in oxidative etching of {100} diamond surface. As for

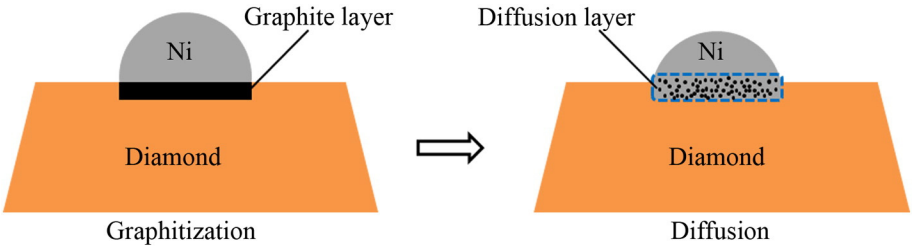

Fig. 7. Schematic model for diamond etching using nickel powder.

{111} planes, similar to diamond etching in O_2/H_2O [19] and potassium nitrate [20], "positive" trigons sided by three {111} walls were formed. Now that the above characteristics are quite different from those in Fig. 1, the synergistic effect of oxygen and nickel on diamond in surface patterning experiment can be excluded.

Based on the aforementioned discussion, it is demonstrated that using carbon black to create a reducing atmosphere for diamond and nickel is an effective method. Even if quite light amount of oxygen existed in the reaction system, its influence on diamond surface patterning process can be ignored.

To explain the diamond etching process, a schematic model is proposed in Fig. 7. At high temperature, diamond surface will be wetted by molten nickel. Under the catalytic effect of nickel, diamond tends to undergo a phase transformation from diamond to graphite. Subsequently, the formed graphitic carbon at the diamond/nickel interface will diffuse into the nickel. Driven by concentration gradient, carbon dissolved in nickel will move to the side away from the interface. Then, the newly exposed nickel in the interface will act on diamond further to keep the etching active. Finally, patterns with certain depth will be formed.

3.5. The pattern area and etch depth on diamond

To evaluate the etch extent of diamond at different temperature, the percentage of pattern area and etch depth on diamond were quantitatively measured. In Fig. 8, it is shown that the pattern area and etch depth on diamond surface increased with elevated temperature. Here, the pattern area reflects the wet degree of diamond by molten nickel. The wetting experiments between iron group metals and graphite stated that they wetted the substrate when their pure forms were used, while they did not wet graphite when metals were pre-saturated with carbon. Likewise, the interaction between iron group metals and diamond was believed to be based on the large solubility of carbon in metals [21]. From the phase diagram of nickel, it is known that the amount of dissolved carbon increases as temperature raises [22]. Consequently, at high temperature diamond surface can be well wetted by nickel leading to the development of large pattern area. While the etch depth can be regarded as an indicator of etch ability of nickel to diamond. Diamond etching process involves the transformation of diamond into graphite and carbon diffusion in molten nickel. The rise of temperature reduced the energy barrier for graphitization and also improved the solubility of carbon in nickel. Hence, at high temperature diamond etching process will be greatly promoted resulting in deeper etch depth. However, since the surface energy of {100} planes is high [23] and its activation energy for graphitization is low, the etch area and depth on {100} planes were larger than those on {111} planes at the same temperature. Finally, at the highest temperature of 950 °C, the average percentages of pattern area and etch depths are 9% and 3.0 μm for {111} planes and 21% and 5.0 μm for {100} planes, respectively.

4. Conclusions

In this work, etch patterns on all the facets of diamond crystallites were achieved by nickel catalytic etching without using flowing gas. Etch patterns formed on {100} planes are a combination of reversed pyramids; while those on {111} planes are hexagons. At the interface of diamond {100} plane and nickel, cubic nanoparticles oriented in ⟨100⟩direction were observed, which may be the result of melting and solidification of eutectic. As temperature rose, the pattern area and etch depth on diamond surfaces trended to increase, and at the same temperature, the pattern area and etch depth on {100} planes were larger than those on {111} planes. At the highest temperature (950 °C), the average percentages of pattern area on {111} and {100} planes are 9% and 21%, and the corresponding etch depths are 3.0 μm and 5.0 μm, respectively. Graphitization was demonstrated to be the dominant mechanism for diamond surface patterning process.

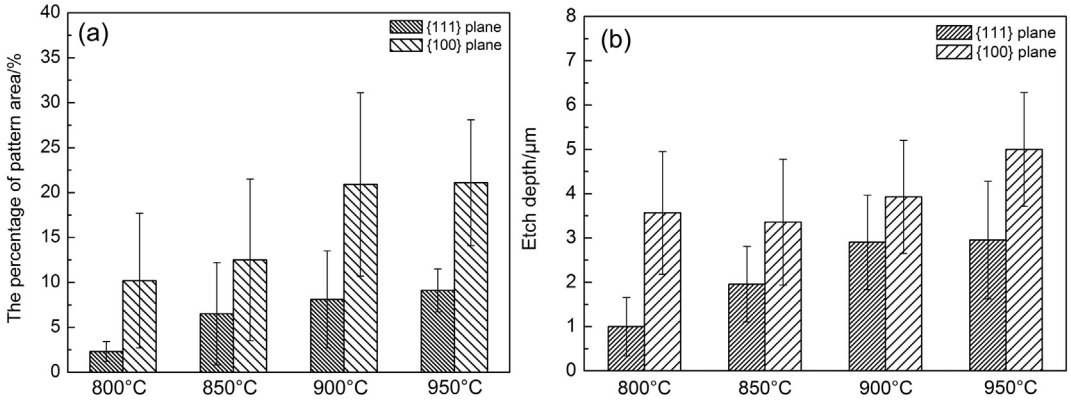

Fig. 8. The pattern area and etch depth on diamond surface.

Prime novelty statement

Diamond crystallites with all planes patterned were achieved without flowing gas. Effects of temperature and orientation on pattern area and etch depth were quantified.

Acknowledgements

The authors would like to acknowledge the financial support from the National Natural Science Foundation of China (Grant No. 51375157). The first author (J. W.) also would like to acknowledge the China Scholarship Council (CSC) for providing her exchange scholarship for Ph.D. study and research at Keio University.

Appendix A. Supplementary data

Supplementary data to this article can be found online at http://dx.doi.org/10.1016/j.diamond.2016.04.010.

References

[1] Y. Zhao, H. Yu, X. Quan, S. Chen, H. Zhao, Y. Zhang, Preparation and characterization of vertically columnar boron doped diamond array electrode, Appl. Surf. Sci. 303 (2014) 419–424.
[2] N. Yang, J. Hees, C.E. Nebel, Diamond ultramicro- and nano-electrode arrays, Novel Aspects of Diamond, Springer 2015, pp. 273–293.
[3] V. Vermeeren, S. Wenmackers, P. Wagner, L. Michiels, DNA sensors with diamond as a promising alternative transducer material, Sensors 9 (2009) 5600–5636.
[4] S.A. Skoog, P.R. Miller, R.D. Boehm, A.V. Sumant, R. Polsky, R.J. Narayan, Nitrogen-incorporated ultrananocrystalline diamond microneedle arrays for electrochemical biosensing, Diam. Relat. Mater. 54 (2014) 39–46.
[5] T. Ohashi, W. Sugimoto, Y. Takasu, Catalytic roughening of surface layers of BDD for various applications, Electrochim. Acta 54 (2009) 5223–5229.
[6] W. Smirnov, J.J. Hees, D. Brink, W. Muller-Sebert, A. Kriele, O.A. Williams, C.E. Nebel, Anisotropic etching of diamond by molten Ni particles, Appl. Phys. Lett. 97 (2010) 073117.
[7] H.-A. Mehedi, C. Hébert, S. Ruffinatto, D. Eon, F. Omnès, E. Gheeraert, Formation of oriented nanostructures in diamond using metallic nanoparticles, Nanotechnology 23 (2012) 455302.
[8] S. Konishi, T. Ohashi, W. Sugimoto, Y. Takasu, Effect of the crystal plane on the catalytic etching behavior of diamond crystallites by cobalt nanoparticles, Chem. Lett. 35 (2006) 1216–1217.
[9] T. Ohashi, W. Sugimoto, Y. Takasu, Catalytic etching of synthetic diamond crystallites by iron, Appl. Surf. Sci. 258 (2012) 8128–8133.
[10] J. Wang, L. Wan, J. Chen, J. Yan, Anisotropy of synthetic diamond in catalytic etching using iron powder, Appl. Surf. Sci. 346 (2015) 388–393.
[11] P.A. Buffat, J.P. Borel, Size effect on the melting temperature of gold particles, Phys. Rev. A 13 (1976) 2287–2298.
[12] B.B. Bokhonov, A.V. Ukhina, D.V. Dudina, K.B. Gerasimov, A.G. Anisimov, V.I. Mali, Towards a better understanding of nickel/diamond interactions: the interface formation at low temperatures, RSC Adv. 5 (2015) 51799–51806.
[13] P.C. Yang, W. Zhu, J.T. Glass, Nucleation of oriented diamond films on nickel substrates, J. Mater. Res. 8 (1993) 1773–1776.
[14] T. Tanaka, N. Ikawa, H. Tsuwa, Affinity of diamond for metals, CIRP Ann. Manuf. Technol. 30 (1981) 241–245.
[15] H. Kanda, T. Ohsawa, O. Fukunaga, I. Sunagawa, Effect of solvent metals upon the morphology of synthetic diamonds, J. Cryst. Growth 94 (1989) 115–124.
[16] L.J. Hardwick, H. Buqa, P. Novák, Graphite surface disorder detection using in situ Raman microscopy, Solid State Ionics 177 (2006) 2801–2806.
[17] F. Tuinstra, J.L. Koenig, Raman spectrum of graphite, J. Chem. Phys. 53 (1970) 1126–1130.
[18] Z. Yuan, Z. Jin, R. Kang, Q. Wen, Tribochemical polishing CVD diamond film with FeNiCr alloy polishing plate prepared by MA-HPS technique, Diam. Relat. Mater. 21 (2012) 50–57.
[19] F. De Theije, E. Van Veenendaal, W. Van Enckevort, E. Vlieg, Oxidative etching of cleaved synthetic diamond {111} surfaces, Surf. Sci. 492 (2001) 91–105.
[20] F.K.D. Theije, O. Roy, N.J.V.D. Laag, W.J.P.V. Enckevort, Oxidative etching of diamond, Diam. Relat. Mater. 9 (2000) 929–934 (926).
[21] A.I. Belyaev, D.B. Butrymowicz, Surface phenomena in metallurgical processes, Springer New York, 1995.
[22] M. Singleton, P. Nash, The C-Ni (carbon-nickel) system, Bull. Alloy Phase Diagr. 10 (1989) 121–126.
[23] W.D. Harkins, Energy relations of the surface of solids I. Surface energy of the diamond, J. Chem. Phys. 10 (1942) 268–272.